

Article

# Tribological Characteristics of Al359/Si3N4/Eggshell Surface Composite Produced by Friction Stir Processing

Ashish Kumar Srivastava <sup>1</sup>, Suryank Dwivedi <sup>2</sup>, Ambuj Saxena <sup>1</sup>, Deepak Kumar <sup>2</sup>, Amit Rai Dixit <sup>2,\*</sup>, Gyanendra Kumar Singh <sup>3</sup>, Javed Khan Bhutto <sup>4</sup> and Rajesh Verma <sup>4</sup>

<sup>1</sup> Department of Mechanical Engineering, G.L. Bajaj Institute of Technology and Management, Greater Noida 201306, Uttar Pradesh, India

<sup>2</sup> Department of Mechanical Engineering, Indian Institute of Technology (ISM), Dhanbad 826004, Jharkhand, India

<sup>3</sup> Department of Mechanical Engineering, School of Mechanical, Chemical and Materials Engineering, Adama Science and Technology University, Adama P.O. Box 1888, Ethiopia

<sup>4</sup> Department of Electrical Engineering, College of Engineering, King Khalid University, Abha 61421, Saudi Arabia

\* Correspondence: amitraidixit@iitism.ac.in

**Abstract:** In the present study, the surface composite Al359/Si3N4/Eggshell is prepared by friction stir processing (FSP). The effect of reinforced particle volume fraction on the microstructural and tribological properties of the Al359/Si3N4/Eggshell surface composites was investigated and compared with the friction stir processed (FSPed) Al359 alloy. The microstructural properties were further investigated by light microscopy, FESEM, and EDS mapping. The tribological properties of the developed composite and FSPed Al359 were investigated using a reciprocating ball-on-plate universal tribometer. The microstructural results showed that defect-free composite surfaces are produced due to improved physical properties, severe plastic deformation, and better grain refinement. Moreover, the mean value of the friction coefficient ( $\mu$ ) for the developed composite and FSPed alloy are  $0.36 \mu$  and  $0.47 \mu$ , respectively. The obtained results indicated that Si<sub>3</sub>N<sub>4</sub>/Eggshell is a promising reinforced particle for improving microstructural and tribological performance in journal bearing, rotors, and machinery applications.

**Keywords:** Al359 alloy; friction stir processing; friction and wear; Si<sub>3</sub>N<sub>4</sub>; eggshell waste; composite structure



**Citation:** Srivastava, A.K.; Dwivedi, S.; Saxena, A.; Kumar, D.; Dixit, A.R.; Singh, G.K.; Bhutto, J.K.; Verma, R. Tribological Characteristics of Al359/Si3N4/Eggshell Surface Composite Produced by Friction Stir Processing. *Coatings* **2022**, *12*, 1362. <https://doi.org/10.3390/coatings12091362>

Academic Editor: Jinyang Xu

Received: 11 August 2022

Accepted: 14 September 2022

Published: 18 September 2022

**Publisher's Note:** MDPI stays neutral with regard to jurisdictional claims in published maps and institutional affiliations.



**Copyright:** © 2022 by the authors. Licensee MDPI, Basel, Switzerland. This article is an open access article distributed under the terms and conditions of the Creative Commons Attribution (CC BY) license (<https://creativecommons.org/licenses/by/4.0/>).

## 1. Introduction

In the past decade, researchers and modern industries have been continuously finding new quality materials that are lightweight, dimensionally accurate, have a high-quality surface finish, a high production rate, are cost-effective to produce, and are environment friendly [1–4]. For these reasons, aluminium alloys and their composites are the primary preference for the aerospace and automotive industries due to their lightweight, good mechanical, and tribological properties [5]. However, the need for specific engineering materials for specific engineering applications is still open to investigation. Aluminium metal matrix composites (AMMCs) have been developed as advanced engineering materials for weight-saving applications in both industries. AMMCs exhibit an excellent combination of high specific strength, hardness, and better wear resistance for various applications. Moreover, the enhancement of all desired properties, such as physical and mechanical, depends on reinforcement/particulates and microstructure [6]. Several researchers have experimented with using different reinforcement particles (SiC, Al<sub>2</sub>O<sub>3</sub>, B<sub>4</sub>C, Gr, TiC, Si<sub>3</sub>N<sub>4</sub>, and TiB<sub>2</sub>, etc.). Si<sub>3</sub>N<sub>4</sub> is considered a standout reinforcement and one of the most promising ceramics because of its high levels of hardness. It also has other extraordinary characteristics, such as low density, high melting point, high thermal stability, and good chemical

stability [7].  $\text{Si}_3\text{N}_4$  also has excellent ballistic and mechanical properties, making it a desirable material for several defence applications [8]. Waste eggshell is a new engineering reinforcement, containing around 95% calcium carbonate ( $\text{CaCO}_3$ ), 3% phosphorus, and signs of magnesium, zinc, sodium, potassium, iron, and copper [9,10]. It can be used as a bio-waste material to meet the different requirements of modern products, and also to create new value. It is an inexpensive reinforcement material with excellent properties, such as low density, hardness, compressive strength, high thermal stability, and it is renewable [11]. These mechanical properties qualify it as an excellent candidate to reinforce aluminium and its alloys, usually used in the automobile industry [12]. Kumar et al. examined the effect of different reinforcement microparticles ( $\text{SiC}$ ,  $\text{Al}_2\text{O}_3$ , and  $\text{Ti}$ ) with the addition of waste carbonized eggshell powder.  $\text{Ti}$ /eggshell base reinforcement in AMMCs obtained an excellent hardness compared to the other reinforcement particles [13]. However, other reinforced composites possess good hardness compared with the base material. The addition of commonly used reinforced particles, such as  $\text{SiC}$ ,  $\text{Al}_2\text{O}_3$ , and  $\text{B}_4\text{C}$ , in the metal matrix improves tensile strength, yield strength, and hardness, but reduces ductility.

Both phase fabrication methods, such as liquid and solid phases, have been successfully used to make the desired composite. Several studies presented the enhancement of the specific mechanical properties and modified the microstructure of the matrix material. However, liquid state processing presents major drawbacks, such as porosity, solute redistribution, and solidification cracking [12–14]. High temperature is required for solid-to-liquid and vapour phase changing processes, but the reverse process (liquid-to-solid phase) reduces some of the special properties of the composites. Several research studies have found that friction stir processing (FSP) is a suitable process for fabricating composites that work in the solid-to-solid state phase, thus eliminating these drawbacks [15,16].

FSP is a technique that has become very popular in recent decades. FSP is a versatile method of solid-state processing, and it is an energy efficient technique that results in no residual stresses that refine the microstructure, densification, and homogeneity of the structure [17,18]. Figure 1a shows the schematic arrangement of FSP. In this process, the matrix material is processed by a non-consumable tool with a shoulder-pin arrangement that rotates at high speed. The friction between the tool and matrix material generates sufficient heat. The tool traverses to cover up the desired area and is stirred by the tool shoulder-pin arrangement in the coverage area. Due to the stirring of the material, severe plastic deformation occurs, which causes refined microstructure, densification, and homogeneity in the formed composites [19,20]. The process parameters can directly control the advantage of FSP on mechanical and microstructural properties. Thus, FSP has manifested a similar or better tribological performance than other conventional processes [21,22].

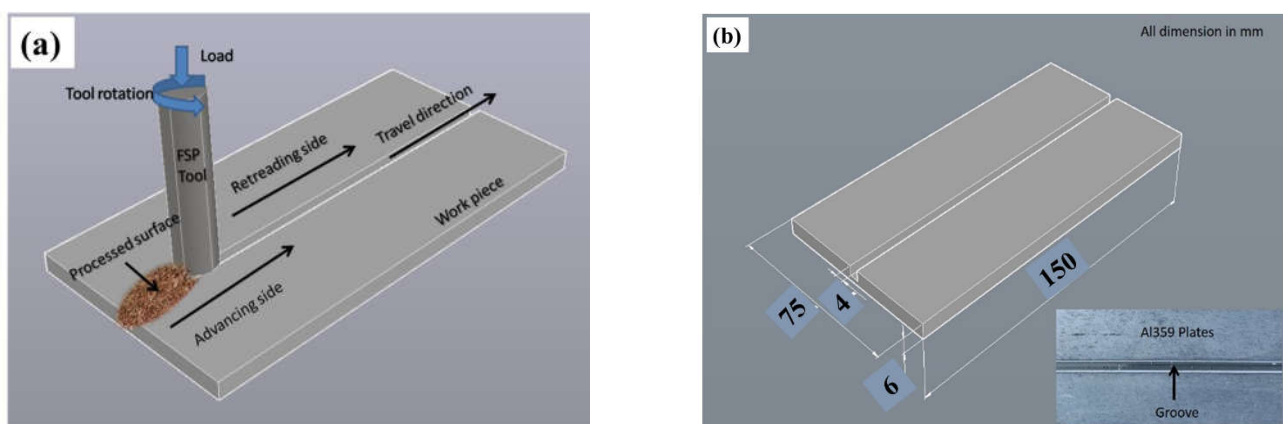


**Figure 1.** Schematic arrangement of the (a) friction stir processing and (b) aluminium alloy AL359 plate.

The focus of the present research is placed on tribological characteristics. Generally, composites demonstrate a high friction coefficient in the range of 0.5–0.8, except for those that slide in water or under other lubricants. In the present work, a vertical milling machine

is used to produce the surface composites. Al359 aluminium alloy was used as a matrix material, while  $\text{Si}_3\text{N}_4$  and waste eggshell powder was used as reinforcement materials (6% by volume). The tribological tests are carried out to test the frictional properties of Al-6%  $\text{Si}_3\text{N}_4$ /Eggshell composites. The microstructural study was done with the help of light microscopy, FE-SEM equipped with EDS mapping.

## 2. Experimental Procedure

Commercially available Al359 aluminium alloy was used as a matrix material. It is a suitable material in applications including aerospace, automotive, and for highly stressed parts (gears, fuse parts, and structural components). Al359 plates were purchased with a dimension of 75 mm  $\times$  150 mm  $\times$  6 mm, as shown in Figure 1b. Before FSP, a square groove was cut transversely from the middle according to the 6% reinforcement volume.  $\text{Si}_3\text{N}_4$  and ball-milled carbonized eggshell powder, each of 3% volume, were selected as the primary and secondary reinforcement. Figure 2a shows the  $\text{Si}_3\text{N}_4$  particle size varying between 5  $\mu\text{m}$  to 80  $\mu\text{m}$  with an average diameter of 18  $\mu\text{m}$ .

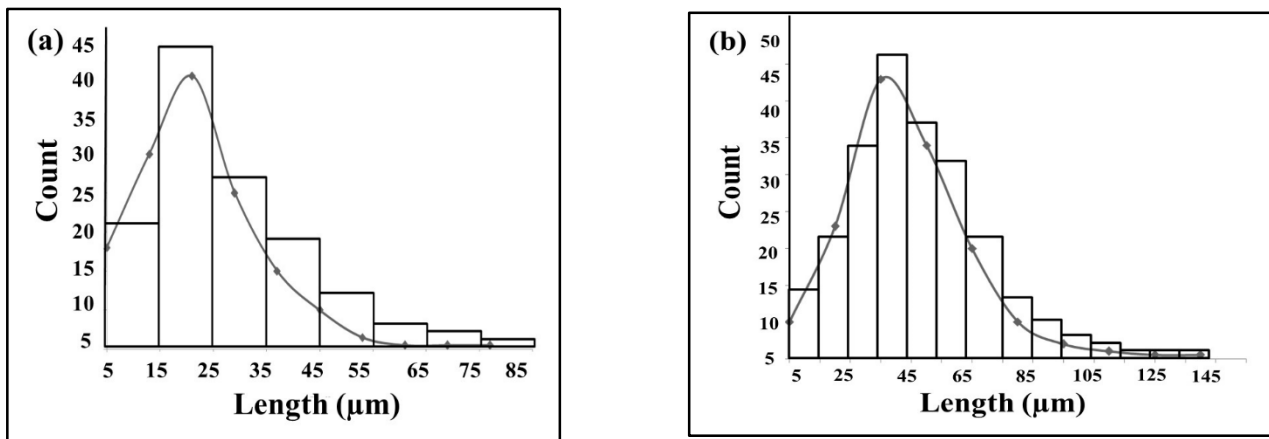


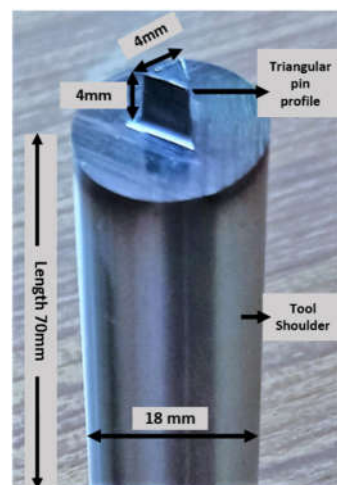
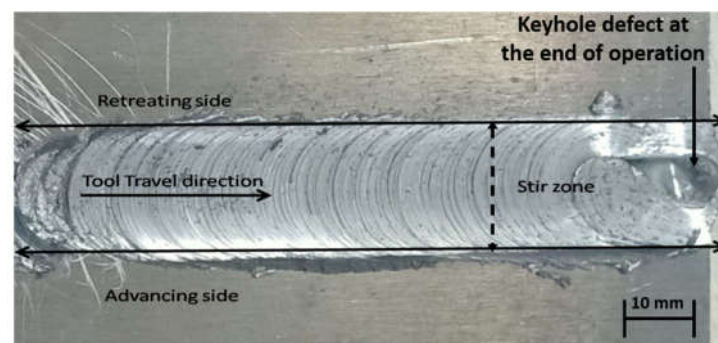
**Figure 2.** The particle size distribution of (a)  $\text{Si}_3\text{N}_4$  particles and (b) eggshell particles.

Waste eggshells were collected from local shops to prepare the carbonized eggshell. They were cleaned to remove any dust and egg liquid. Next, they were solar-dried for 48 h to remove the moisture. Dry eggshells were preheated to a temperature of 1000  $^{\circ}\text{C}$  for 1 h. Carbonized eggshells were ball milled to obtain a fine powder. The obtained powder was passed through multiple sieves of the required size to ensure that particles in the correct range were obtained [23]. Figure 2b showed the eggshell particle size varying between 5  $\mu\text{m}$  to 140  $\mu\text{m}$  with an average diameter of 33  $\mu\text{m}$ . Previous research and lab experimentations have found that the process parameters of FSP affect the mechanical and physical properties of the developed composites. Parameters, such as rotational tool speed, traverse speed, tilt angle, and axial force, can improve the properties of the composites. The preferred process parameters for fabricating Al359/ $\text{Si}_3\text{N}_4$ /Eggshell surface composites are given in Table 1, and are based on the pilot experiments and the authors' own previous published literature.

**Table 1.** Process parameters used in the fabrication of Al359/Si<sub>3</sub>N<sub>4</sub>/Eggshell surface composites.

Process Parameters	Values
Rotational speed (rpm)	2250
Transverse speed (mm/min)	25
Tool Tilt angle (°)	2
Shoulder diameter (mm)	18
Axial Pressure (kN)	8
Pin profile of the tool	Triangular
Pin length (mm)	4
Pin edges (mm)	4

A non-consumable HSS tool with a shoulder diameter of shoulder 18 mm, shoulder length of 70 mm, and a triangular profile pin with 4 mm edges were prepared as shown in Figure 3. To make the homogeneous mixture, 3% of both types of reinforcements were chosen and mixed manually after preheating to 350 °C. The homogeneous preheated mixture of Si<sub>3</sub>N<sub>4</sub>/Eggshell powder (6% by volume) was filled into the square groove (dimensions are decided based on the 6% volume of reinforcement material) made on the top surface of the base plate. A pin-less HSS tool was used to cover the reinforcement powder to prevent it from spurting out of the track during the FSP processing. Then the primary FSP process was carried out using a vertical milling machine at room temperature, and within the process parameters described in Table 1, and with 6% volume of the reinforcement material. Figure 4 shows Al359/Si<sub>3</sub>N<sub>4</sub>/Eggshell surface composite after the FSP.

**Figure 3.** Photographic view of the HSS tool used in the experiment.**Figure 4.** Photographic view of Al359/Si<sub>3</sub>N<sub>4</sub>/Eggshell surface composite after FSP.

The friction stir processed (FSPed) samples were cut using the Wire-EDM (CNC wire-cut electric discharge machine manufactured by Electronica Machine Tool Ltd, IIT ISM

Dhanbad, India) and polished in the YZ plane using SiC paper of grit size 600 grade (230 × 280 mm) to remove uneven surfaces.

For the microstructural study, rectangular cross-section of the specimens was obtained as per the ASTM-E3 standard. Further, it was polished with diamond paste and etched in a solution of Keller's reagent (15 mL HCL + 25 mL HNO<sub>3</sub> + 10 mL HF + 50 mL H<sub>2</sub>O). The microstructure of the specimens was studied through inverted light microscope (manufacturer Leica- model- DMI3000 M, IIT ISM Dhnabad, India) and FE-SEM (Jeol jsm-7800 prime field emission scanning electron microscopy) coupled with an EDS detector (LN<sub>2</sub> Free SDD X-max 80 energy dispersive detector). The sliding wear behaviour of the FSPed Al359/Si<sub>3</sub>N<sub>4</sub>/Eggshell sample and FSPed Al359 without any reinforcement were studied using a reciprocating-type ball-on-plate universal tribometer (MFT 5000, Rtec instruments, USA). The 2D schematic of the used tribometer setup is depicted in Figure 5. Before the tribological analysis, specimens were prepared as per the ASTM G99 standard procedures. The samples were cut and cleaned in isopropyl alcohol solution for 10 min, followed by deionized water. The ultrasonically cleaned samples were dried in a furnace at 100 °C to remove the moisture from the samples' surface. The reciprocating-type ball-on-plate wear mode was set to perform the tribological analysis, and a stainless steel ball (6 mm diameter) was used as a counter body. Thus, a sliding pair of Al359/Si<sub>3</sub>N<sub>4</sub>/Eggshell and a stainless steel 316 ball worked as a working pair. During the sliding wear tests, a 2 Hz frequency was set to achieve the sliding velocity of 10 mm/s. A 15 N load and 5 mm stroke length were applied for the test duration of 10 min. The average coefficient of friction (COF) and frictional force (F<sub>x</sub>) for the Al359/Si<sub>3</sub>N<sub>4</sub>/Eggshell composite sample was obtained as per the ASTM standard G115 for the sliding wear test. Thereafter, to remove worn-out debris, the samples were ultrasonically cleaned and dried in the furnace (Stericox, India) at 100 °C temperature for 30 min. Further, the 3D images of the worn samples were captured and studied in detail to study the wear mechanism.

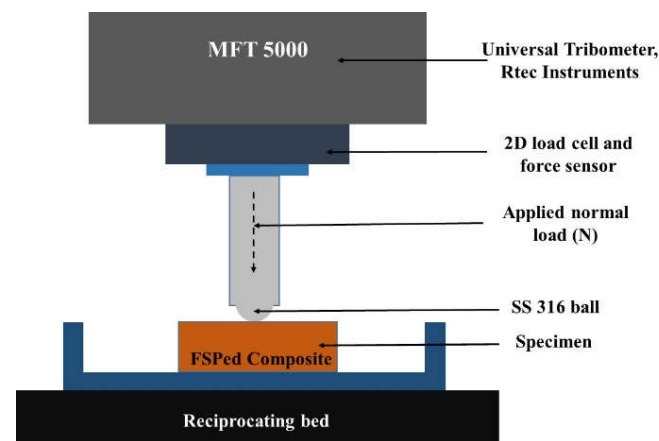


**Figure 5.** 2D Schematic arrangement of the ball-on-plate tribometer for the friction and wear test of Al359/Si<sub>3</sub>N<sub>4</sub>/Eggshell sample against the SS316 steel ball.

### 3. Results and Discussion

The microstructures of the FSPed specimen were observed using light microscopy, as shown in Figure 6a,b taken at two different locations (a) stir zone (SZ) (b) thermomechanical affected zone (TMAZ). The matrix phase of the alloy is shown by the brighter regions, and the reinforcement phase is shown by the darker regions in the micrograph. From Figure 6, it can be seen that reinforced particles are dispersed homogeneously with a minor porosity due to the high tool rotation. Moreover, the distribution of the reinforced particles is more homogeneous with the reduced density, which decreases the porosity in the sample. When compared to the base alloy, the larger grains break into smaller sized grains with the increased number of the grain boundary. The result shows that the FSPed zone produces a

defect-free composite that can offer excellent mechanical, physical, and plastic deformation and better grain refinement.

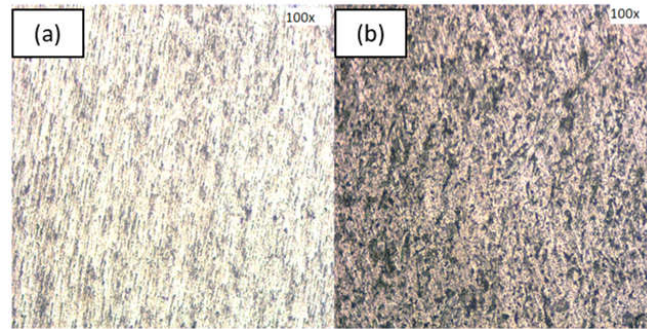


**Figure 6.** Optical photomicrograph of Al359/Si<sub>3</sub>N<sub>4</sub>/Eggshell surface composites. (a) stir zone (SZ) (b) thermomechanical affected zone (TMAZ).

Morphological studies of the FSPed sample were done using FESEM, which was coupled with EDS mapping. This was used to produce a detailed study of the microstructure, plastic deformation, grain refinement, and chemical composition of the composite. The SEM micrograph of the FSPed composite at different magnifications and different locations of stir zone at 10  $\mu$ m, TMAZ location at 1  $\mu$ m and 10  $\mu$ m) is presented in Figure 7a–d, respectively. The obtained micrograph depicted the severe plastic deformation of the base alloy and the presence of a reinforcement phase in the stir zone region and TMAZ. A fine-grained structure with a large number of grain boundaries was formed, which is attributed to the dynamic recrystallization during the FSP process. The optimized parameters were used to produce the equiaxed and refined grain structure, which highlights the capability of FSP processing. It is revealed from the FESEM images that a uniform distribution of the Si<sub>3</sub>N<sub>4</sub>/Eggshell reinforced particles was obtained. The desired composites, consisting of matrix material and reinforced particles, have fine and smooth surfaces caused by the FSP with proper shoulder design. However, few defects, such as clustering of the reinforcement phase and micro-pores, can be seen in the micrographs. These defects can be considered negligible due to the enhanced microstructural features. The chemical composition of the Al359/Si<sub>3</sub>N<sub>4</sub>/Eggshell developed surface composites is presented in Figure 8a,b.

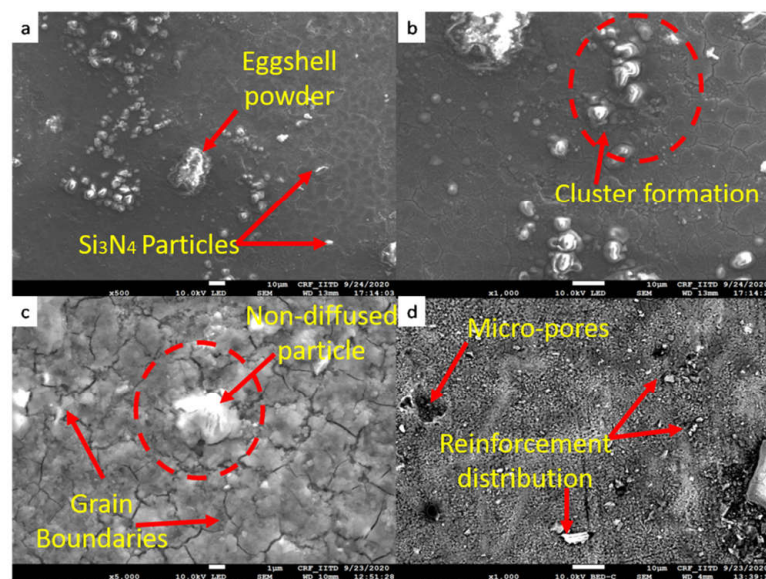
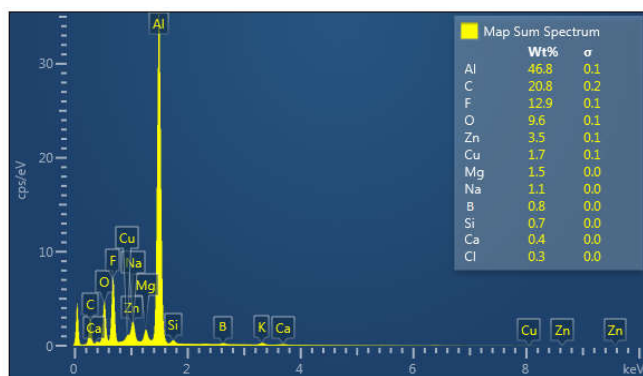
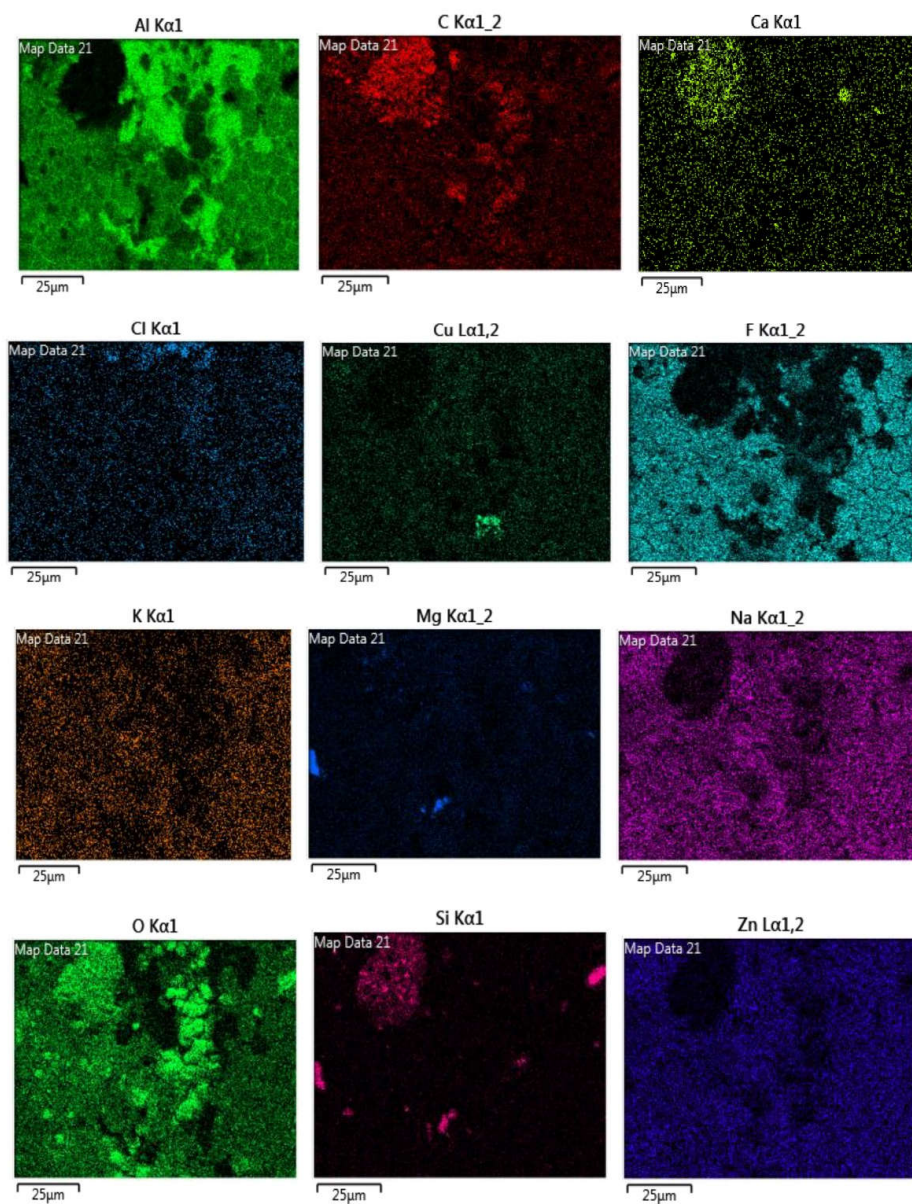


**Figure 7.** FE-SEM micrograph of Al359/Si<sub>3</sub>N<sub>4</sub>/Eggshell surface composites. (a) stir zone location 1 at 10  $\mu$ m; (b) stir zone location 2 at 10  $\mu$ m (c) TMAZ location 1  $\mu$ m (d) TMAZ location 10  $\mu$ m.



(a)



(b)

**Figure 8.** (a) EDS spectrum of Al359/Si<sub>3</sub>N<sub>4</sub>/Eggshell surface composites. (b) EDS phase mapping of Al359/Si<sub>3</sub>N<sub>4</sub>/Eggshell surface composites.

Figure 8a shows the EDS spectrum and Figure 8b shows the element mapping of the composition of surface composite Al359/Si<sub>3</sub>N<sub>4</sub>/Eggshell. The EDS spectrum of all the major constituents of the developed composite, such as Al, Si, and Ca, can be seen in the elemental list along with their significant weight percentage. The small contribution of other constituents of base alloy Al359, such as Zn, Cu, and Mg, are also present in the selected phase of the EDS mapping. It is evident from Figure 8b that the major elements of Al359/Si<sub>3</sub>N<sub>4</sub>/Eggshell surface composite, such as Zn, Cu, Mg, and Ca, are completely diffused with the Al matrix material. This is because, during the FSP, the frictional heat plastically deformed the aluminium matrix material below its melting temperature, resulting in a softening of the matrix. In this region, it can be concluded that proper wettability formed between the reinforced particles and matrix material. However, the Si phase is seen in low density. This is attributed to the fact that the Si<sub>3</sub>N<sub>4</sub> particles are not completely diffused into the matrix material due to their low density and high melting temperature. Some other elements, i.e., carbon, oxygen, and fluorine, also showed they can exist in the matrix material due to chemical and metallurgical reactions during the preparation of the composites by FSP.

Further, the sliding wear test was carried out using the ball-on-plate reciprocating-type universal tribometer. During the test, a constant normal load of 15 N and sliding speed of 10 mm/s were used to evaluate the friction and wear performance of the developed surface composites. A frictional force ( $F_x$ ) and normal force ( $F_z$ ) were measured during the test run. The 2D load cell was used to maintain the normal force ( $F_z$ ) of  $15\text{ N} \pm 1\text{ N}$  during the test, which can be seen in Figure 9. Furthermore, a coefficient of friction (COF) value was calculated as a function of time from the force data set and presented in Figure 10.

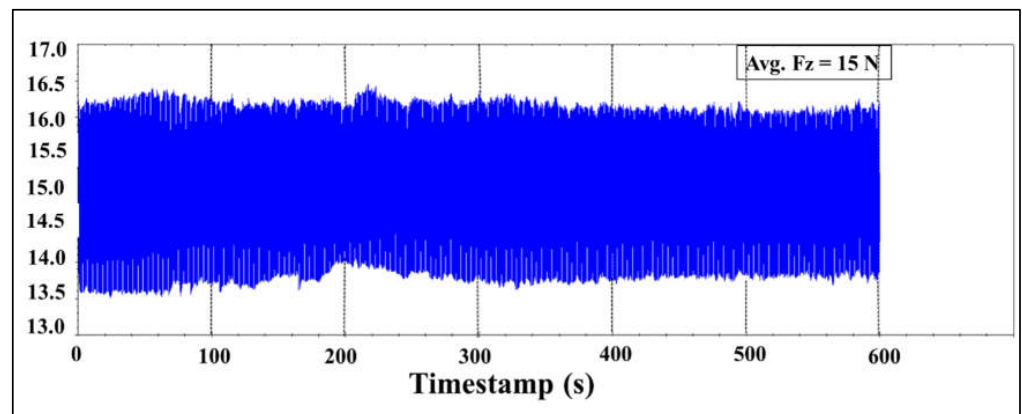


Figure 9. Generation of normal force ( $F_z$ ) graph for Al359/Si<sub>3</sub>N<sub>4</sub>/Eggshell surface composites.

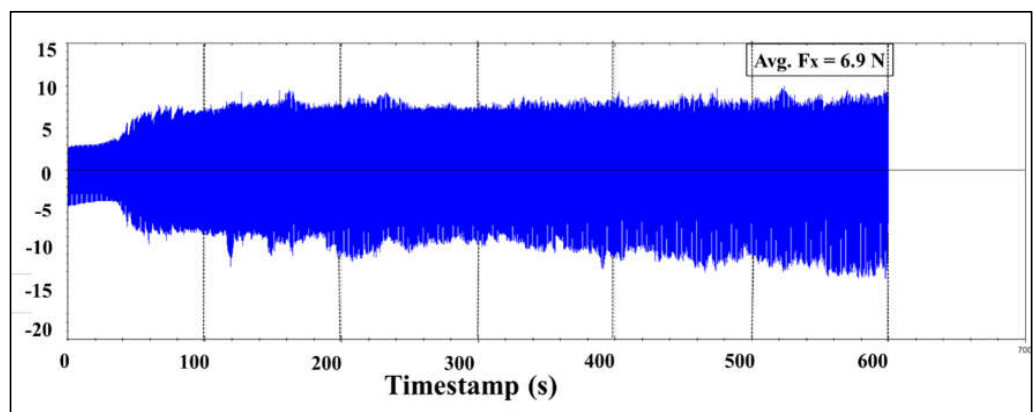
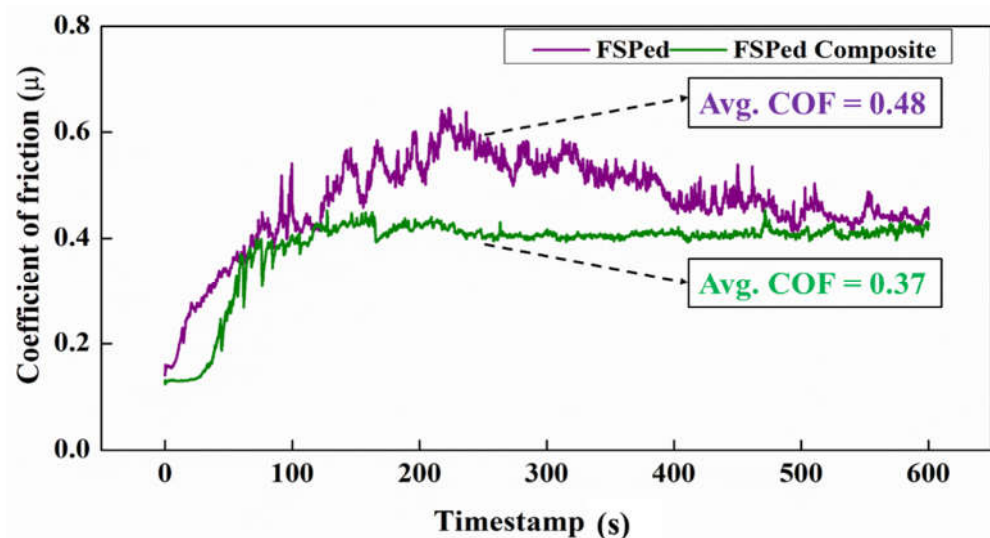


Figure 10. Generation of the friction force ( $F_x$ ) graph for Al359/Si<sub>3</sub>N<sub>4</sub>/Eggshell surface composites.



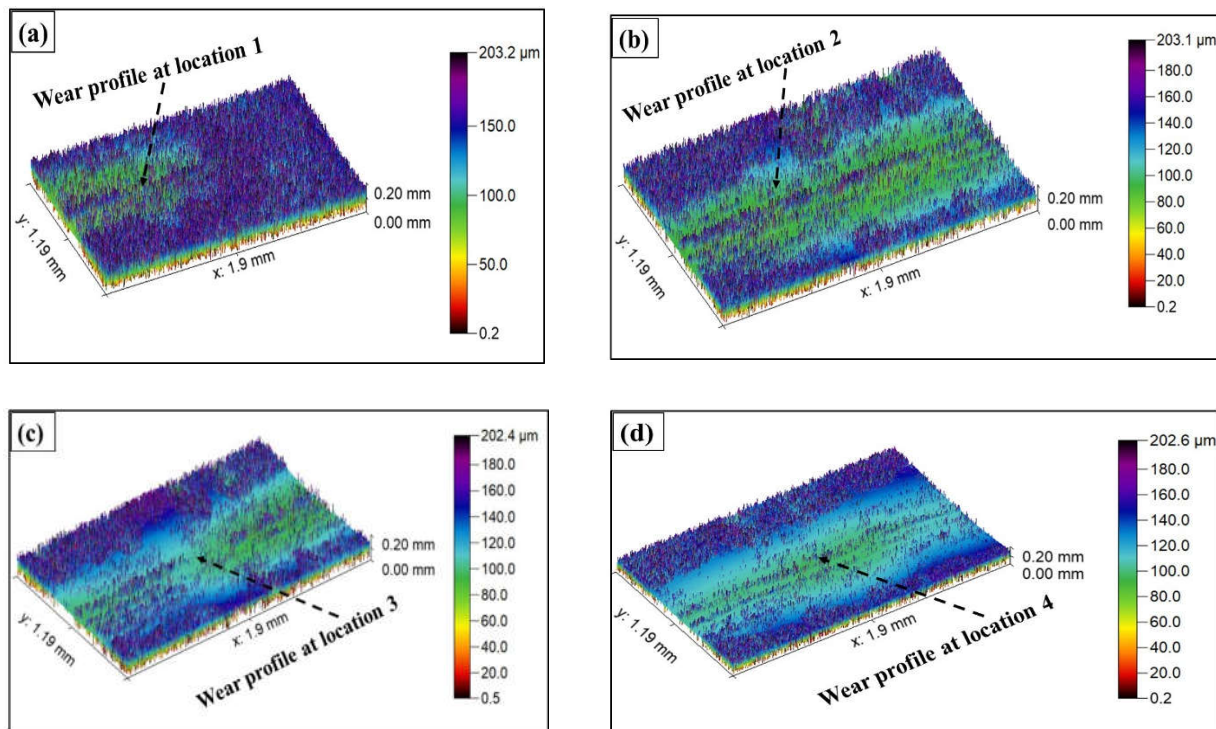
Figure 9 highlights the generation of the frictional force ( $F_x$ ) value for the composite surface. At the beginning of the process, the generation of the frictional force value is low, but later on it increases and stabilizes (Figure 10). The average  $F_x$  value for the composite surface is 6.9 N. Further, Figure 11 depicts the COF ( $\mu$ ) values for both the FSPed Al359 without reinforcement and Al359/Si<sub>3</sub>N<sub>4</sub>/Eggshell surface composite. During the test, the COF value for the surface composite steadily increased during the first 80 s, and then continued to rise until approximately 170 s, where it reached roughly 0.42  $\mu$ . Afterwards, the COF value was reduced and stabilized at 0.39  $\mu$ . The mean value of the COF for the produced composite was 0.37. Furthermore, for the FSPed Al359 without reinforcement, the COF increases at a higher rate than the composite surface, and attains an average COF value of 0.48  $\mu$  (Figure 11), which dictates the poor tribological performance of the FSPed material. The tribological results show that the COF value for the surface composite is 23% lower than the FSPed Al359 without reinforcement. Moreover, the variation in friction coefficient with time was observed for the FSPed sample, with greater variation during the first 80 s, influenced by the “stick-slip” phenomena. This effect can occur when objects are analysed while in the dynamic contact between two surfaces, resulting in a spontaneous jerking motion and unstable movement along the sliding track. However, during the dynamic contact, a significant increase in the friction force and friction coefficient was observed due to the unevenness that comes from the developed surface material and the counter body (SS316L ball). This unevenness causes a specific roughness value, piloting to an insignificant contact surface between the ball and the plate, which leads to the separation of the soft particle from the mating surface. However, it should also be noted that the decrease in friction coefficient is mainly caused by a growth of an adhesion layer of the reinforced particles, and due to the formation of the uniform fine grain structure in the stir zone.



**Figure 11.** Generation of COF with sliding time for FSPed and Al359/Si<sub>3</sub>N<sub>4</sub>/Eggshell surface composites.

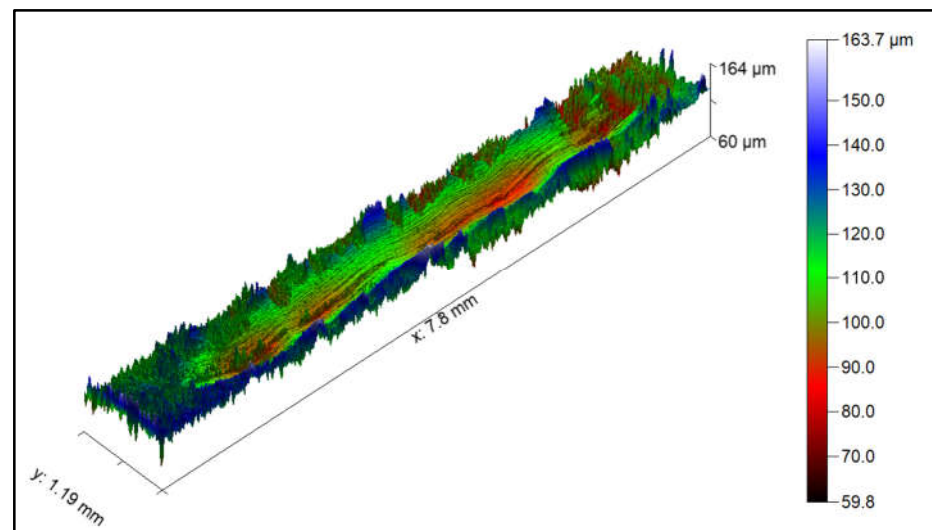
The EDX (Figure 8a) and elemental mapping (Figure 8b) results show the presence of oxygen and carbon elements that dictate the presence of oxides and carbides over the composite surfaces. The modified elemental composition helps to increase the hardness of the prepared surface composite [24]. However, according to the Pascal Law, it is known that the wear resistance property is directly proportional to the hardness value of that sample [25]. The increased surface hardness leads to improved tribological performance, as can be seen in Figure 11. Therefore, the obtained results help to understand the tribological performance of the composite surfaces and presents the relationship between the mechanical, microstructural, and tribological performance of the Al359/Si<sub>3</sub>N<sub>4</sub>/Eggshell composite and FSPed Al359 alloy.

Figure 12a–d shows the 3D images of the tribological wear track on Al359/Si<sub>3</sub>N<sub>4</sub>/Eggshell surface composites during the reciprocating ball-on-plate test. The worn-out depth profile was captured, as per the given ASTM standard G133-05. The 3D profiles were captured at five different locations to study the generation of the wear depth. During the wear test, the applied normal force (15 N) ensured continuous contact between the mating surfaces, thus producing friction and leading to the generation of the wear-out profiles. Figure 12a shows the lack of uniformity of the wear track due to increased amplitude values, which refers to an increase in volatility during the initial timestamp. A tribolayer is formed with a discontinuous layer, with a small amount of debris and material ruptures because these particles have mechanically adhered to the surface. Figure 12b shows the formation of a continuous layer due to the rapid growth of the temperature in the contact area. Both friction forces and temperature conditions favour the Al alloy's adhesive phenomena to reinforcement material. Figure 12c shows the adhered layered became unstable and possibly detached due to the reaction of friction forces on the wear surface. Figure 12d reveals the continuous layer and the dynamic behaviours of the adhesion wear mechanism.



**Figure 12.** 3D image of the tribological wear track on FSPed composites during the ball-on-plate wear test as per the ASTM standard G133-05 at five different locations. (a) location 1; (b) Location 2 (c) Location 3 (d) Location 4.

The red colours in Figure 13 shows the formed valley in the wear track. The reinforced (Si<sub>3</sub>N<sub>4</sub>/Eggshell) particles are adhered by the Al alloy layer's wear, which accelerates the worn particles over the surface. Due to this impact, debris from Al alloy and reinforced particles (hard particles) is again deposited on the wear track and produces improved frictional properties. In recent years, individually customized products have gained favour, and the design of suitable composite materials has become more flexible for various applications, such as aerospace and automobiles. The results show that friction stir processing can be a promising approach for producing such components using Al359/Si<sub>3</sub>N<sub>4</sub>/Eggshell composites with improved physical properties.



**Figure 13.** 3D image of the tribological wear track on FSPed composites during the reciprocation ball-on-plate wear test.

#### 4. Conclusions

In this study, an Al359/Si<sub>3</sub>N<sub>4</sub>/Eggshell surface composite was fabricated by friction stir processing at room temperature. The microstructural results confirm the uniform and homogeneous distribution of Si<sub>3</sub>N<sub>4</sub>/Eggshell throughout the stir zone. The FESEM images show that the FSPed region has refined grains and a large number of grain boundaries due to severe plastic deformation, leading to better tribological properties. The tribological study reveals that the mean friction coefficient values for the FSPed Al359 without reinforcement and Al359/Si<sub>3</sub>N<sub>4</sub>/Eggshell surface composite specimens are 0.48  $\mu$  and 0.37  $\mu$ , respectively, which proves the improved frictional properties of the composite surface. The tribological results show that the COF value for the surface composite is 23% lower than that of FSPed Al359 without reinforcement. In addition to being a replacement for surface modification, the surface composite may be used to improve friction performance above and beyond traditional surface modification techniques. The obtained results indicate that Si<sub>3</sub>N<sub>4</sub>/Eggshell is a promising reinforced particle for the improvement of microstructural and tribological performance in journal bearing, rotors, and machinery applications.

**Author Contributions:** Conceptualization, A.K.S., and S.D.; methodology, S.D., A.S.; software, A.S., D.K.; validation, A.R.D., A.K.S., and G.K.S.; formal analysis, A.K.S., and S.D.; writing—A.K.S., and S.D., supervision, A.R.D.; funding acquisition, J.K.B. and R.V. All authors have read and agreed to the published version of the manuscript.

**Funding:** This research was funded by Javed Khan Bhutto and Rajesh Verma, grant number RGP 2/91/43. The APC was funded by [King Khalid University, Saudi Arabia].

**Institutional Review Board Statement:** Not applicable.

**Informed Consent Statement:** Not applicable.

**Data Availability Statement:** Not applicable.

**Acknowledgments:** The authors extend their appreciation to the Deanship of Scientific Research at King Khalid University, Saudi Arabia, for funding this work through the Research Group Program under Grant No: RGP 2/91/43.

**Conflicts of Interest:** The authors declare no conflict of interest.

## References

1. Srivastava, A.K.; Dixit, A.R.; Maurya, M.; Saxena, A.; Maurya, N.K.; Dwivedi, S.P.; Bajaj, R. 20<sup>th</sup> century uninterrupted growth in friction stir processing of lightweight composites and alloys. *Mater. Chem. Phys.* **2021**, *266*, 124572. [[CrossRef](#)]
2. Dwivedi, R.; Srivastava, A.K.; Singh, R.K. Effect of eggshell waste and B<sub>4</sub>C particles on the mechanical and tribological properties of Al7075 alloy developed by friction stir processing. *Metall. Res. Technol.* **2022**, *119*, 508. [[CrossRef](#)]
3. Dwivedi, R.; Singh, R.K.; Kumar, S.; Srivastava, A.K. Parametric optimization of process parameters during the friction stir processing of Al7075/SiC/waste eggshell surface composite. *Mater. Today Proc.* **2021**, *47*, 3884–3890. [[CrossRef](#)]
4. Srivastava, A.K.; Kumar, N.; Dixit, A.R. Friction stir additive manufacturing—An innovative tool to enhance mechanical and microstructural properties. *Mater. Sci. Eng. B* **2021**, *263*, 114832. [[CrossRef](#)]
5. Rajawat, M.S.; Pagrut, S.; Dwivedi, S.; Raj, R.; Dixit, A.R. Microstructural characterization of Friction stir assisted laminated lap welding of AA6063 sheets. *Mater. Today Proc.* **2022**, *56*, 949–953. [[CrossRef](#)]
6. Kurt, A.; Uygur, I.; Cete, E. Surface modification of aluminium by friction stir processing. *J. Mater. Process. Technol.* **2011**, *211*, 313–317. [[CrossRef](#)]
7. Srivastava, A.K.; Maura, N.K. Experimental investigation of A359/Si<sub>3</sub>N<sub>4</sub> surface composite produced by multi-pass friction stir processing. *Mater. Chem. Phys.* **2021**, *257*, 123717. [[CrossRef](#)]
8. Srivastava, A.K.; Maurya, M.; Saxena, A.; Maurya, N.K.; Dwivedi, S.P.; Dixit, A.R. Microstructural and fractographic analysis of A359/Si<sub>3</sub>N<sub>4</sub> surface composite produced by friction stir processing. *Int. J. Mater. Res.* **2021**, *112*, 68–77. [[CrossRef](#)]
9. Srivastava, A.K.; Saxena, A.; Dixit, A.R. Investigation on the thermal behaviour of AZ31B/waste eggshell surface composites produced by friction stir processing. *Compos. Commun.* **2021**, *28*, 100912. [[CrossRef](#)]
10. Srivastava, A.K.; Kumar, N.; Saxena, A.; Tiwari, S. Effect of friction stir processing on microstructural and mechanical properties of lightweight composites and cast metal alloys—A review. *Int. J. Cast Met. Res.* **2021**, *34*, 169–195. [[CrossRef](#)]
11. Bahrami, A.; Soltani, N.; Pech-Canul, M.I.; Gutiérrez, C.A. Development of metal matrix composites from industrial/agricultural waste materials and their derivatives. *Crit. Rev. Environ. Sci. Technol.* **2016**, *46*, 143–208. [[CrossRef](#)]
12. Dwivedi, R.; Kumar Singh, R.; Kumar Srivastava, A.; Anand, A.; Kumar, S.; Pal, A. Statistical optimization of process parameters during the friction stir processing of Al7075/Al<sub>2</sub>O<sub>3</sub>/waste eggshell surface composite. In *Recent Trends in Industrial and Production Engineering*; Springer: Singapore, 2021; pp. 107–118. [[CrossRef](#)]
13. Kumar, S.; Srivastava, A.K.; Singh, R.K. Fabrication of AA7075 Hybrid Green Metal Matrix Composites by Friction Stir Processing Technique. *Ann. Chim. Sci. Matériaux* **2020**, *44*, 295–300. [[CrossRef](#)]
14. Yuvaraj, N.; Aravindan, S. Fabrication of Al5083/B<sub>4</sub>C surface composite by friction stir processing and its tribological characterization. *J. Mater. Res. Technol.* **2015**, *4*, 398–410. [[CrossRef](#)]
15. Karpasand, F.; Abbasi, A.; Ardestani, M. Effect of amount of TiB<sub>2</sub> and B<sub>4</sub>C particles on tribological behaviour of Al7077/TiB<sub>2</sub>/B<sub>4</sub>C mono and hybrid surface composites produced by friction stir processing. *Surf. Coat. Technol.* **2020**, *390*, 125680. [[CrossRef](#)]
16. Kumar, S.; Srivastava, A.K.; Singh, R.K.; Dwivedi, S.P. Experimental study on hardness and fatigue behavior in joining of AA5083 and AA6063 by friction stir welding. *Mater. Today Proc.* **2020**, *25*, 646–648. [[CrossRef](#)]
17. Thankachan, T.; Prakash, K.S. Micro structural mechanical and tribological behaviour of aluminium nitride reinforced copper surface composites fabricated through friction stir processing route. *Mater. Sci. Eng. A* **2017**, *688*, 301–308. [[CrossRef](#)]
18. Ma, Z.Y. Friction stir processing technology: A review. *Metall. Mater. Trans. A* **2008**, *39*, 642–658. [[CrossRef](#)]
19. Mishra, R.S.; Ma, Z.Y.; Charit, I. Friction stir processing; a novel technique for fabrication of surface composite. *Mater. Sci. Eng. A* **2003**, *341*, 307–310. [[CrossRef](#)]
20. Sharma, V.; Gupta, Y.; Kumar, V.M.; Prakash, U. Friction stir processing strategies for uniform distribution of reinforcement in a surface composite. *Mater. Manuf. Process.* **2015**, *31*, 1384–1392. [[CrossRef](#)]
21. Mostafapour, A.; Khandani, S.T. Role of hybrid ratio in microstructural, mechanical and sliding wear properties of the Al5083/Graphite/Al<sub>2</sub>O<sub>3</sub> a surface hybrid nanocomposite fabricated via friction stir processing method. *Mater. Sci. Eng. A* **2013**, *559*, 549–557. [[CrossRef](#)]
22. Sahu, P.S.; Banchhor, R. Effect of silicon carbide reinforcement on wear and tribological properties of aluminium matrix composites. *Int. J. Innov. Sci. Eng. Technol.* **2015**, *3*, 293–299.
23. Singh, R.K.; Srivastava, A.K.; Singh, D.K. Microstructural and X-ray Diffraction Analysis of Surface Composite AZ31b/MgO/B<sub>4</sub>C Produced by Friction Stir Processing. In *Recent Trends in Industrial and Production Engineering*; Lecture Notes in Mechanical Engineering; Dwivedi, A., Sachdeva, A., Sindhvani, R., Sahu, R., Eds.; Springer: Singapore, 2022. [[CrossRef](#)]
24. Prakash, O.; Dwivedi, S.; Pagrut, S.; Rajawat, M.S.; Raj, R.; Srivastava, A.K.; Dixit, A.R. Investigation on the friction stir assisted lap joining of pure copper and aluminium 6063 alloy. *Mater. Today Proc.* **2022**, *62*, 398–403. [[CrossRef](#)]
25. Dwivedi, S.; Dixit, A.R.; Das, A.K.; Adamczuk, K. Additive texturing of metallic implant surfaces for improved wetting and biotribological performance. *J. Mater. Res. Technol.* **2022**, *20*, 2650–2667. [[CrossRef](#)]